# An Asymptotic Framework for Fox's H-Fading Channel with Application to Diversity-Combining Receivers

PUSPRAJ SINGH CHAUHAN[1], SANDEEP KUMAR[2], *SENIOR MEMBER, IEEE*, ANKIT JAIN[1], AND LAJOS HANZO[3], *LIFE FELLOW, IEEE*

***Abstract*—Unified statistics are valuable in the performance analysis of communication systems. In this context, Fox's H-function has been shown to be eminently suitable for diverse scenarios. Another pivotal requirement is to have a low computational complexity, which is often hard to achieve for generalized models. Given this motivation, in this article we have presented high-power, low-complexity solutions for the outage probability (OP) and the average symbol error probability (SEP). Additionally, diversity techniques are harnessed for mitigating the effect of fading, which are then analysed based on the results derived. The entire methodology is governed by the origin probability density function rather than approximating the performance metrics under high-power. All the presented mathematical expressions are compared and validated through computer simulations (Monte-Carlo) to verify the accuracy of the proposed framework.**

## I. Introduction

Given the availability of generalised distributions like $\alpha$-$\mu$, $\eta$-$\mu$, $\kappa$-$\mu$, $\alpha$-$\eta$-$\mu$, $\alpha$-$\eta$-$\mu$, $\alpha$-$\kappa$-$\mu$, etc., the need for having unified statistics is increasing day by day. In this context, Fox's H-function has grown in popularity because of its versatile nature and elegant form in terms of representing most of the earlier proposed fading channels [1]. The distribution offers significant flexibility in characterizing numerous fading models [2, Table I].The measurement and modeling campaigns have evidenced that the multipath fading of the V2V channel at 5 GHz and 5.2 GHz can be closely modelled by the generalized Fox's H-function distribution. The model encompasses the various other typical models of vehicular and D2D propagation scenarios such as Rayleigh, Nakagami-$m$, Fisher-$F$ (at 5.8 GHz for D2D application), Weibull etc. [3], [4], [5].

Various researchers have proposed novel frame-works for analysing the performance of wireless systems relying on Fox's H-fading [1], [2], [6]–[10]. In this regard, Yilmaz *et al.* [6] has presented a methodology for deriving the closed-form expressions of the average BEP and average capacity for transmission over the Hyper Fox's H-fading model expressed in terms of Fox's H-function. The evaluation of the average BEP and average capacity expressions routinely utilize the MGF based approach for both single and multiple links. In [7], [8], the channel capacity is derived both with and without delay constraints for different adaptive schemes relying on optimal rate adaptation, on optimal power, on channel inversion, and on truncated channel inversion at a fixed rate over Fox's H-fading channel. Abo Rahama *et al.* [1] derived novel results for the PDF and CDF over the sum of Fox's H-function utilizing the MGF-based approach. They also utilized these results for evaluating the OP, average BEP, and ergodic capacity of wireless system. Physical layer statistics have been presented for transmission over Fox's H wiretap fading channel in [9], where the eavesdropper may be colluding or non-colluding. In case of a colluding scenario, the eavesdropper is equipped with MRC and SC schemes. The validity of the proposed formulation has been verified under different fading environments. The results presented in [9] subsumed the results presented in previous treatises. Furthermore, El Ayadi [2] and Chauhan *et al.* [10] derived cognitive radio performance metrics for transmission over Fox's H-fading under different propagation environments. In [1], [2], [6]–[10] the performance metrics relied either on univariate, bivariate, or multivariate Fox's H-functions. However, the earlier analytics may limit the operating range due to instabilities, while evaluating these expressions by numerical integration. Furthermore, they may fail to provide a visual interpretation of how the system reacts to time-variant changes in channel and system characteristics. Therefore, it is usually desired to find simpler expressions for the quantities of interest.

To address these concerns, the research community turned to asymptotic analysis at high SNR [11]–[14]. This approach results in computational simplicity and allows us to analyse the variations of statistics by relying on the average SNR. It also helps in comparing the performance of various modulation schemes. This approach has been frequently invoked [1], [2], [10]–[14]. Specifically, the asymptotic results derived for various metrics are discussed both for SISO and SIMO scenarios [1], [2], [10]. The high-power expressions of the average bit error or symbol error probabilities are evaluated in [1]. Similarly, the average probability of detection and average area under the receiver's operating characteristic curve are also derived in [1].

1 - Department of Electronics & Communication Engineering, Pranveer Singh Institute of Technology, Kanpur, India

2 - Central Research Laboratory, Bharat Electronics Limited, Gaziabad, India

3 - School of Electronics and Computer Science, University of Southampton, Southampton SO17 1BJ, U.K.

L. Hanzo would like to acknowledge the financial support of the Engineering and Physical Sciences Research Council projects EP/W016605/1 and EP/X01228X/1 as well as of the European Research Council's Advanced Fellow Grant QuantCom (Grant No. 789028)

TABLE I
NOMENCLATURE.

| | |
|---|---|
| 5G | Fifth Generation |
| A2G | Air-to-Ground |
| ALN | Additive Laplacian Noise |
| AWGN | Additive White Gaussian Noise |
| $\alpha$-$\mu$/G | $\alpha$-$\mu$/Gamma |
| BEP | Bit Error Probability |
| BFSK | Binary Frequency Shift Keying |
| BPSK | Binary Phase-Shift Keying |
| CDF | Cumulative Distribution Function |
| D2D | Device-to-Device |
| DSS | Double Shadowed Scenario |
| EGC | Equal Gain Combining |
| EGK | Extended Generalized-$K$ |
| EG-G | Extended Generalized Gamma |
| F-S | Fisher-Snedecor |
| G2A | Ground-to-Air |
| GBK | Generalised Bessel-$K$ |
| GK | Generalised-$K$ |
| i.i.d. | Independent and Identically Distributed |
| i.n.i.d. | Independent and Non-Identically Distributed |
| LT | Laplace Transform |
| MED | Minimum Euclidian Distance |
| MGF | Moment-Generating Function |
| MIMO | Multiple-Input Multiple-Output |
| MRC | Maximum-Ratio Combining |
| OP | Outage Probability |
| PAM | Pulse Amplitude Modulation |
| PDF | Probability Density Function |
| PSK | Phase-Shift Keying |
| QoS | Quality-of-Service |
| QPSK | Quadrature Phase Shift Keying |
| RMS | Root-Mean-Square |
| Rx | Receiver |
| SAGIN | Space-Air-Ground Integrated Network |
| SC | Selection Combining |
| SEP | Symbol Error Probability |
| SIMO | Single-Input Multiple-Output |
| SISO | Single-Input Single-Output |
| SNR | Signal-to-Noise Ratio |
| SSS | Single Shadowed Scenario |
| Tx | Transmitter |
| V2V | Vehicle-to-Vehicle |

TABLE II
NOTATIONS

| | |
|---|---|
| $\alpha$ | Non-linearity parameter |
| $\mu$ | Number of multipath cluster |
| $\gamma$ | Instantaneous received SNR |
| $\bar{\gamma}$ | Average received SNR |
| $\hat{r}$ | Fading figure of EG-G distribution |
| $\xi$ | Shaping factor of EG-G distribution |
| $\hat{r}_s$ | Shadowing severity of EG-G distribution |
| $\xi_s$ | Shadowing inhomogeneity of EG-G distribution |
| $\Gamma(.)$ | Gamma function |
| $\hat{n}$ | Fading severity of F-S $F$ distribution |
| $\hat{m}$ | Shadowing severity of F-S $F$ distribution |
| $n_G$, $m_G$, & $\hat{\lambda}$ | Shaping factors of GBK distribution |
| $\delta$ | Path loss exponent |
| $D$ | Tx and Rx separation |
| $\hat{k}$ | Shape parameter for Gamma distribution |
| $\hat{\Omega}$ | Average power of $\alpha$-$\mu$ distribution |
| $m_i$, $\{i=1,2\}$ | Nakagami-$m$ fading parameters |
| $a_i$, $\{i=1,2\}$ | Shaping parameter of Inverse Gamma distribution |
| $\tilde{m}_i$ & $\tilde{m}_{si}$, $\{i=1,2\}$ | Shape parameters of GK distribution |
| $P_t$ | Transmitted power |
| $E$ | Instantaneous propagation loss |
| $N_0$ | Noise power |
| $\Omega_{si}$,$\{i=1,2\}$ | Mean power of GK distribution |
| $\tilde{\xi}$ | Ratio of equivalent beam radius and pointing error displacement standard deviation at the Rx |
| $r$ | Detection parameter for Gamma-Gamma distribution |
| $\varsigma$ & $\varpi$ | Scintillation parameters of the atmospheric turbulence |
| $\mu_{R_D}$ | average SNR for Gamma-Gamma distribution |
| $L$ | Number of independent parallel paths |
| $\gamma_r$ | $r^{th}$ branch instantaneous received SNR |
| $M_{\gamma_r}(s)$ | MGF of $r^{th}$ branch instantaneous received SNR |
| $\gamma_{MRC}$ | Instantaneous received SNR at the output of MRC detector |
| $\gamma_{EGC}$ | Instantaneous received SNR at the output of EGC detector |
| $\gamma_{SC}$ | Instantaneous received SNR at the output of SC detector |
| $M_{X_r}(s)$ | MGF of $r^{th}$ branch envelope |
| $f_Y(\gamma)$ | PDF of received SNR |
| $F_{\gamma_r}(\gamma)$ | $r^{th}$ branch CDF |
| $\gamma_{th}$ | Threshold SNR |
| $P_{out}(.)$ | Probability of outage |
| $erfc(.)$ | Complementary error function |
| $P_e(.)$ | Instantaneous SEP |
| $\bar{P}_e$ | Average SEP |

The recent works on the asymptotic analysis over Fox H-fading channels have been listed in Table 1. Although, the asymptotic analysis of different system performance metrics was presented for Fox H-fading channels, most of the analysis was carried out for single-branch Rxs. Only [1] has considered the asymptotic analysis of Fox H-fading channels for MRC diversity, but the results derived are not in generic form. Explicitly, the average SEP expressions were found using Eq. (13) of [15], which is only applicable for BPSK and BFSK. The asymptotic outage and ergodic capacity expressions do not rely on simple functions, but due to the presence of multiple summation terms required for MRC diversity, substantial computation is required for their evaluation. Furthermore, it is noted from Table 1, that none of the previous contributions have analysed EGC and SC diversity for Fox H-fading channels. Although EGC is suboptimal, it benefits from simpler channel estimation, which only requires estimation of the channel phase, but not the channel amplitude [16]. Due to the complex circuitry of the MRC, the EGC is often preferred in 5G applications, including V2V and D2D communication. Hence the asymptotic analysis of Fox H-fading channel is the need of the hour. Furthermore, none of the previous works have considered Laplacian noise in their analysis, which is essentially used for satisfying the differential privacy that prevents information leakage in secure applications, indoor, outdoor, free-space optics and undersea communication environments [17]–[21].

In an attempt to fill these knowledge gaps, we have carried out the asymptotic analysis of Fox-H fading channels for various diversity combining techniques. The application of the resultant formulas in deriving the generic expressions of the performance metrics has been demonstrated. We have considered both the ubiquitous AWGN and ALN. By contrast, the

TABLE III
CONTRASTING OUR CONTRIBUTIONS TO THE LITERATURE OF FOX H-FADING CHANNELS

| Parameters | [1] | [2] | [9] | [10] | [22] | [23] | [24] | [25] | [26] | This work |
|---|---|---|---|---|---|---|---|---|---|---|
| i.i.d. Branches | | | | | ✓ | | | ✓ | ✓ | ✓ |
| i.n.i.d. Branches | ✓ | | | | | | | | | ✓ |
| MRC diversity | ✓ | | | | | | | ✓ | ✓ | ✓ |
| Outage probability | ✓ | | | | ✓ | | ✓ | | | ✓ |
| Average SEP | ✓ | | | | | | ✓ | | ✓ | ✓ |
| Effective capacity | | | | | | ✓ | | | | |
| Ergodic capacity | ✓ | | | | | | ✓ | | ✓ | |
| Physical Layer Security parameters | | | ✓ | | ✓ | | | | | |
| Spectrum sensing parameters | | ✓ | | ✓ | | | | ✓ | | |
| Diversity gain | | | | ✓ | | | | | | ✓ |
| AWGN | ✓ | ✓ | ✓ | ✓ | ✓ | ✓ | ✓ | ✓ | ✓ | ✓ |
| Laplacian noise | | | | | | | | | | ✓ |
| Origin PDF-based approach | | | | ✓ | | | | ✓ | ✓ | ✓ |
| Function approximation under High SNR-based approach | ✓ | ✓ | ✓ | | ✓ | ✓ | ✓ | | | |
| EGC diversity | | | | | | | | | | ✓ |
| SC diversity | | | | | | | | | | ✓ |

system considered here has multiple Rx antennas along with diverse combining schemes such as MRC, EGC, and SC. In this treatise, we have focused on a PDF-based approach. The main contributions of this work are summarised as follows:

• New expressions are derived for different diversity combining techniques, relying on both i.i.d and independent as well as on non-identically distributed branches.

• Explicitly, analytical expressions are derived for both the OP and for the average SEP. Furthermore, unified error probability statistics are obtained for both coherent and non-coherent schemes in AWGN scenarios. Additionally, the error probability of coherent modulation schemes is evaluated in the face of ALN.

• The final BER and OP expressions are articulated with the aid of computationally convenient asymptotes. Simulations are conducted to validate the accuracy of the results produced, which are accurate at high-SNRs.

The results derived here are beneficial as they (i) yield a unified mechanism for the average SEP and OP associated with multiple branches; (ii) serve as an efficient potential tool for analysing the system performance, when the channel characteristics are acquired by Fox's H module or in the analysis of special cases, which have hitherto not been taken into consideration. For easy referencing, all the acronyms and variables used throughout the work are defined in Table I and Table II, respectively.

The rest of the paper is organised as follows: In Section 2, the general Fox channel model is covered in detail, and a few unique Fox H-fading channel examples are taken into consideration. The methodology of handling different diversity schemes is elaborated on in Section 3. In Section 4, asymptotic results are provided for the OP and the average SEP under both AWGN and ALN scenarios. Section 5 verifies the accuracy of the results. Finally, Section 6 summarizes the paper.

## II. FOX'S H-FADING CHANNEL

In the literature, Fox's H representation is often used to characterize the channels in wireless propagation environments [1], [2], [10], because it subsumes well-known distributions modelling the practical propagation channels [6]. These channels include the Rayleigh, Maxwell, Weibull, Gamma, Weibull, Nakagami-$m$, GK, EGK, EG-G, F-S-$F$, Nakagami-$m$/Gamma, scenarios as their special cases [2], [6], [9]. The model's practical utility can be found in a variety of applications, including vehicle-to-vehicle and keyhole MIMO systems [3], [27], G2A, and A2G unmanned aerial vehicle communications [28], millimeter-wave (i.e. $\geq$ 60 GHz) & free space optical communication [29], as well as D2D scenarios of indoor and outdoor environments [5]. Let the statistical variation of these real-world wireless communication environments follow Fox's H representation. Then the instantaneous power PDF is expressed as [2, equation (10)]

$$f_Y(\gamma) = \mathcal{R} H_{\hat{p},\hat{q}}^{\hat{m},\hat{n}} \left[ \mathcal{T}\gamma \middle| \begin{matrix} (e_j,E_j)_{j=1..\hat{p}} \\ (f_j,F_j)_{j=1..\hat{q}} \end{matrix} \right], \ \gamma > 0, \tag{1}$$

where the parameters $\hat{m}$, $\hat{n}$, $\hat{p}$, $\hat{q}$ posses positive integer values, and follow $0 \leq \hat{m} \leq \hat{q}$, $0 \leq \hat{n} \leq \hat{p}$. The constants $\mathcal{R}$ and $\mathcal{T}$ in (1) are adjusted to satisfy that $\int_0^\infty f_Y(\gamma) d\gamma$=1. Equation (1) can alternatively be written in integral form as [30, equations. (1.2) & (1.3)]

$$\begin{aligned} f_Y(\gamma) &= \frac{\mathcal{R}}{2\pi i} \int_{\mathcal{L}} \Theta_{\hat{p},\hat{q}}^{\hat{m},\hat{n}} \left[ s \middle| \begin{matrix} (e_j,E_j)_{j=1..\hat{p}} \\ (f_j,F_j)_{j=1..\hat{F}} \end{matrix} \right] (\mathcal{T}\gamma)^{-s} ds, \\ &= \frac{\mathcal{R}}{2\pi i} \int_{\mathcal{L}} (\mathcal{T}\gamma)^{-s} \\ &\times \frac{\prod_{j=1}^{\hat{m}} \Gamma(f_j + F_j S) \prod_{j=1}^{\hat{n}} \Gamma(1 - e_j - E_j s)}{\prod_{j=\hat{n}+1}^{\hat{p}} \Gamma(e_j + E_j s) \prod_{j=\hat{m}+1}^{\hat{q}} \Gamma(1 - f_j - F_j S)} ds, \end{aligned} \tag{2}$$

where $E_j > 0$ for $j$=1,...$\hat{p}$ and $F_j > 0$ for $j$=1,...$\hat{q}$ and the path of integration will be governed by the function's parameters. The $f_Y(\gamma)$ expressions are illustrated in Table IV for the Maxwell, $\alpha$-$\mu$, EG-G [6], F-S-$\mathcal{F}$ [9], GBK, $\alpha$-$\mu$/G, SSS, DSS, cascaded G-$K$, Gamma-Gamma, N*Rayleigh, N*Nakagami-$m$, N*GK, N*Fisher, and N*$\alpha$-$\mathcal{F}$ models for ground-to-ground and A2G channels. The values of $\mathcal{R}$ and $\mathcal{T} > 0$ from the table may be determined for different fading

models. Explicitly, in Table IV, we can see some special cases of Fox's H-fading models, which have already been introduced in the literature, such as the Maxwell, $\alpha$-$\mu$ [9, Table I], E G-G [6, Table II], F-S $\mathcal{F}$ [9, Table I], and N*$\alpha$-$\mathcal{F}$ [31] distributions. But others, such as, GBK is deduced by utilizing [32, equation (8.4.23.1)] and [30, equations (1.59-1.60)] on [33, equation (1)]. Fox's H-function is derived for $\alpha$-$\mu$/G distributions by following [30, equation (1.60)] and [34, equation (7)], for DSS from [36, equation (7)], for SSS from [36, equation (10)], for cascaded G-$K$ from [35, equation (18)], while for N*Rayleigh from [38], for N*Nakagami-$m$ from [39], for N*GK from [40], and for N*Fisher distributions from [41], which are derived with the aid of [32, equation (8.3.2.21)] and then [30, Property 1.3 & 1.5]. Finally, Fox's H for Gamma-Gamma distribution [37] is deduced with the aid of [32, equation (8.3.2.21)] and [30, Property 1.4, 1.3, & 1.5].

## III. Asymptotic Analysis

Asymptotic analysis has gained special attention during the past few years in system optimization [11]. In the literature, different methodologies are proposed for analysing the system performance attained at both low and high power, as detailed below:

In [11], Zhang *et al.* proposed a new asymptotic analysis framework, in which the PDF is first approximated around the origin and then different performance metrics are evaluated. This approach is well suited for most distributions, but it faces difficulties in diversity analysis associated with distributions having summation terms, as exemplified by the Mixture-Gamma [42], Weibull/Log-normal [43], and Mixture-Inverse Gaussian [44], [45] distributions. Peppas *et al.* [46] proposed asymptotic solutions for cognitive radio scenarios by approximating the results at high power, but their solutions exhibited limitations both when the PDF has a complex mathematical structure, and for spatial diversity techniques.

Additionally, asymptotic frameworks are capable of reducing the analytical complexity of diversity reception. The conventional approaches rely on the PDF at the origin, followed by averaging and using the AWGN and ALN contamination to derive the asymptotic expressions of the OP, average SEP, and average probability of detection. As a benefit, Fox's H-fading model will resolve the issues stated above. When $Z \to 0$ the expression given by (1), will have the structure given as [47, Corollary 3]

$$\mathcal{R}H_{\hat{p},\hat{q}}^{\hat{m},\hat{n}}\left[\mathcal{T}Z\right]_{Z\to 0} = \mathcal{R}h_j(\mathcal{T}Z)^{\Omega}, \tag{3}$$

where $\Omega = min_{1\le j\le \hat{m}}\left[\frac{Re(f_j)}{F_j}\right]$ and $h_j$ is evaluated using [47, Corollary 2] and is defined as

$$h_j = \frac{\prod_{i=1,i\neq j}^{\hat{m}}\Gamma\left(f_i - \frac{f_jF_i}{F_j}\right)\prod_{i=1}^{\hat{n}}\Gamma\left(1-e_i+\frac{f_jE_i}{F_j}\right)}{F_j\prod_{i=\hat{n}+1}^{\hat{p}}\Gamma\left(e_i-\frac{f_jE_i}{F_j}\right)\prod_{i=\hat{m}+1}^{\hat{q}}\Gamma\left(1-f_i-\frac{f_jF_i}{F_j}\right)}, \tag{4}$$

where $h_j$ is listed in Table V for various Fox's H-fading channels. In the cases, where $\hat{m}$>1, $h_j$ has numerous values, which hence requires the selection of the most appropriate parameters. The CDF of the expression given by (3) is evaluated by employing the identity $F_Y(\gamma) = \int_0^{\gamma} f_Y(\gamma)d\gamma$ and it is given by

$$F_Y(\gamma) = \frac{\mathcal{R}h_j\mathcal{T}^{\Omega}}{\Omega+1}\gamma^{\Omega+1}. \tag{5}$$

### A. Diversity Analysis of Fox's H-Distribution

In a communication system, the spurious effect of fading is often compensated by the inclusion of multiple antennas at the Tx or at the Rx or both, so that the QoS can be maintained. Various signal combining techniques are utilised in the open literature to improve the QoS. Among them, MRC, EGC, and SC are the most popular diversity schemes. The most complex MRC yields the best improvements, followed by EGC and SC. In this subsection, we highlight the PDF expressions of the above diversity schemes.

*1) MRC diversity PDF:* The MRC scheme combines the signal received from independent paths, which are first co-phased, then weighted by a corresponding weighting factor inversely proportional to their SNR, and finally added improve the instantaneous SNR of the combiner output. The MRC output may then be expressed as [48]

$$\gamma_{MRC} = \sum_{r=1}^{L}\gamma_r. \tag{6}$$

Taking the LT of (6), yields

$$M_{\gamma_{MRC}}(s) = \prod_{r=1}^{L}M_{\gamma_r}(s). \tag{7}$$

The MGF for the individual branch SNR is calculated by taking the LT of (3) with the aid of [49, Eq. 3.381.4], as given by

$$M_{\gamma}(s) = \mathcal{R}h_j\mathcal{T}^{\Omega}\frac{\Gamma(\Omega+1)}{s^{\Omega+1}}. \tag{8}$$

Substituting (8) into (7) and after some further algebraic manipulations, we arrive at:

$$M_{\gamma_{MRC}}(s) = \left\{\prod_{r=1}^{L}\mathcal{R}_rh_j\mathcal{T}^{\Omega_r}\Gamma(\Omega_r+1)\right\}\frac{1}{s^{\left(\sum_{r=1}^{L}\Omega_r\right)+L}}. \tag{9}$$

Upon multiplying the numerator and denominator of (9) by $\Gamma\left(\left(\sum_{r=1}^{L}\Omega_r\right)+L\right)$ and then taking the inverse LT, we get the desired origin PDF expression of

$$f_{\gamma_{MRC}}^{inid}(\gamma) = \mathcal{K}^{MRC}\gamma^{\Psi^{MRC}-1}, \tag{10}$$

where the parameters $\mathcal{K}^{MRC}$ and $\Psi^{MRC}$ are defined in Table VI. Upon assuming $L$ i.i.d. branches, and $\bar{\gamma_1}$=$\bar{\gamma_2}$=.....=$\bar{\gamma_L}$=$\bar{\gamma}$, (7) may be reformulated as

$$M_{\gamma_{MRC}}^{iid}(s) = \left[M_{\gamma_r}(s)\right]^L. \tag{11}$$

Upon substituting (8) into (11) and then employing the inverse LT, one obtains the origin PDF under the i.i.d. case associated with the same structure as given in (10). The respective parameters are illustrated in Table VI. In Fig. 1 the Fisher-Snedecor $F$ origin power PDF is compared to the exact power

TABLE IV
UNIQUE DISTRIBUTION EXAMPLES OF FOX'S H-FUNCTION.

| Channel | $f_Y(\gamma)$ |
|---|---|
| Maxwell [2, Table I] | $f_Y(\gamma) = \frac{3}{\sqrt{\pi}\bar{\gamma}} H_{0,1}^{1,0}\left[\frac{3\gamma}{2\bar{\gamma}}\Big|_{(\frac{1}{2};1)}^{-}\right]$ |
| $\alpha$-$\mu$ [9, Table I] | $f_Y(\gamma) = \frac{\mu^{\frac{2}{\alpha}}}{\Gamma(\mu)\bar{\gamma}} H_{0,1}^{1,0}\left[\frac{\mu^{\frac{2}{\alpha}}\gamma}{\bar{\gamma}}\Big|_{(\mu-\frac{2}{\alpha};\frac{2}{\alpha})}^{-}\right]$, $\alpha$>0 & $\mu$>0 |
| EG-G [6, Table II] | $f_Y(\gamma) = \frac{\beta\beta_s}{\Gamma(\hat{r})\Gamma(\hat{r}_s)\bar{\gamma}} H_{0,2}^{2,0}\left[\frac{\beta\beta_s}{\bar{\gamma}}\gamma\Big|_{(\hat{r}-\frac{1}{\xi},\frac{1}{\xi}),(\hat{r}_s-\frac{1}{\xi_s},\frac{1}{\xi_s})}^{-}\right]$, $\beta$=$\Gamma(\hat{r}+1/\xi)/\Gamma(\hat{r})$ & $\beta_s$=$\Gamma(\hat{r}_s+1/\xi_s)/\Gamma(\hat{r}_s)$ |
| F-S $\mathcal{F}$ [9, Table I] | $f_Y(\gamma) = \frac{\hat{n}}{\hat{m}\Gamma(\hat{n})\Gamma(\hat{m})\bar{\gamma}} H_{1,1}^{1,1}\left[\frac{\hat{n}\gamma}{\hat{m}\bar{\gamma}}\Big|_{(\hat{n}-1,1)}^{(-\hat{m},1)}\right]$ |
| GBK [33] | $f_Y(\gamma) = \frac{1}{\Gamma(m_G)\Gamma(n_G)\Xi} H_{0,2}^{2,0}\left[\frac{\gamma}{\Xi}\Big|_{(m_G-\frac{1}{\hat{\lambda}};\frac{1}{\hat{\lambda}})\ (n_G-\frac{1}{\hat{\lambda}};\frac{1}{\hat{\lambda}})}^{-\quad -}\right]$, $\Xi$=$\frac{\bar{\gamma}\Gamma(m_G)\Gamma(n_G)}{\Gamma(m_G+1/\hat{\lambda})\Gamma(n_G+1/\hat{\lambda})}$ |
| $\alpha$-$\mu$/G [34] | $f_Y(\gamma) = \frac{\mu^{\frac{1}{\alpha}} D^{\delta}}{\Gamma(\mu)\Gamma(\hat{k})v\hat{\Omega}} H_{0,2}^{2,0}\left[\frac{\mu^{\frac{1}{\alpha}} D^{\delta}\gamma}{v\hat{\Omega}}\Big|_{(\mu-\frac{1}{\alpha},1)(\hat{k}-1,1)}^{-}\right]$, 2<$\delta$<6 |
| SSS [36] | $f_Y(\gamma) = \frac{\mathcal{A}_1 m_1 m_2}{\bar{\gamma}} H_{1,2}^{2,1}\left[\frac{m_1 m_2\gamma}{\bar{\gamma}}\Big|_{(m_1-1,1)(m_2-1,1)}^{(-a_1,1)}\right]$, $\mathcal{A}_1$=$\frac{1}{\Gamma(m_1)\Gamma(m_2)\Gamma(a_1)}$ |
| DSS [36] | $f_Y(\gamma) = \frac{\mathcal{A}_2 m_1 m_2}{\bar{\gamma}} H_{2,2}^{2,2}\left[\frac{m_1 m_2\gamma}{\bar{\gamma}}\Big|_{(m_1-1,1)(m_2-1,1)}^{(-a_2,1)(-a_1,1)}\right]$, $\mathcal{A}_2$=$\frac{1}{\Gamma(m_1)\Gamma(m_2)\Gamma(a_1)\Gamma(a_2)}$ |
| Cascaded G-$K$ [35] | $f_Y(\gamma) = \mathcal{A}_3\mathcal{A}_4 H_{0,4}^{4,0}\left[\mathcal{A}_4\gamma\Big|_{(\tilde{m}_{s1}-1,1)(\tilde{m}_1-1)(\tilde{m}_{s2}-1,1)(\tilde{m}_2-1)}^{-}\right]$, $\mathcal{A}_3 = \frac{1}{\Gamma(\tilde{m}_1)\Gamma(\tilde{m}_2)\Gamma(\tilde{m}_{s1})\Gamma(\tilde{m}_{s2})}$ $\mathcal{A}_4 = \frac{\tilde{m}_1\tilde{m}_2\tilde{m}_{s1}\tilde{m}_{s2}}{\bar{\gamma}}$ & $\bar{\gamma} = \frac{P_t E}{N_0}\Omega_{s1}\Omega_{s2}$ |
| Gamma-Gamma [37] | $f_Y(\gamma) = \frac{(\varsigma\varpi)^r \tilde{\xi}^2}{\mu_{R_D}\Gamma(\varsigma)\Gamma(\varpi)} H_{1,3}^{3,0}\left[\frac{(\varsigma\varpi)^r}{\mu_{R_D}}\gamma\Big|_{(\tilde{\xi}^2-r,r)(\varsigma-r,r)(\varpi-r,r)}^{(\tilde{\xi}^2+1-r,r)}\right]$ |
| N*Rayleigh [38] | $f_Y(\gamma) = \frac{1}{\bar{\gamma}} H_{0,N}^{N,0}\left[\frac{\gamma}{\bar{\gamma}}\Big|_{(0,1)(0,1)----(0,1)}^{-}\right]$ |
| N*Nakagami-$m$ [39] | $f_Y(\gamma) = \frac{1}{\bar{\gamma}} H_{0,N}^{N,0}\left[\frac{\gamma}{\bar{\gamma}}\prod_{i=1}^{N}\Gamma(m_i)\Big|_{(m_1-1,1)(m_2-1,1)--(m_N-1,1)}^{-}\right]$ |
| N*GK [40] | $f_Y(\gamma) = \frac{\prod_{i=1}^{N}\tilde{m}_i\tilde{m}_{si}}{\bar{\gamma}\prod_{i=1}^{N}\Gamma(\tilde{m}_i)\Gamma(\tilde{m}_{si})} H_{0,2N}^{2N,0}\left[\prod_{i=1}^{N}\frac{\Gamma(\tilde{m}_i)\Gamma(\tilde{m}_{si})\gamma}{\bar{\gamma}}\Big|_{(\tilde{m}_1-1,1)(\tilde{m}_{s1}-1,1)----(\tilde{m}_N-1,1)(\tilde{m}_{sN-1},1)}^{-}\right]$ |
| N*Fisher [41] | $f_Y(\gamma) = \frac{1}{\bar{\gamma}\prod_{i=1}^{N}\Gamma(\hat{n}_i)\Gamma(\hat{m}_i-1)} H_{N,N}^{N,N}\left[\frac{\gamma}{\bar{\gamma}}\prod_{i=1}^{N}\frac{\Gamma(\hat{n}_i)}{\Gamma(\hat{m}_i-1)}\Big|_{(\hat{n}_1-1,1)(\hat{n}_2-1,1)----(\hat{n}_N-1,1)}^{(-\hat{m}_1,1)(-\hat{m}_2,1)---(-\hat{m}_N,1)}\right]$ |
| N*$\alpha$-$\mathcal{F}$ [31] | $f_Y(\gamma) = \frac{1}{\prod_{i=1}^{N}\Theta_i^{\frac{2}{\alpha_i}}\bar{\gamma}_i\Gamma(\mu_i)\Gamma(\hat{m}_i)} H_{N,N}^{N,N}\left[\frac{\gamma}{\prod_{i=1}^{N}\Theta_i^{\frac{2}{\alpha_i}}\bar{\gamma}_i}\Big|_{\Upsilon_1,\Upsilon_2,-----\Upsilon_N}^{\Phi_1,\Phi_2,-----\Phi_N}\right]$, $\Phi_i = (1-\hat{m}_i-2/\alpha_i, 2/\alpha_i)$ $\Theta_i = \frac{\hat{m}_i-1}{\mu_i}$ and $\Upsilon_i = (\mu_i-2/\alpha_i, 2/\alpha_i)$ |

PDF for different fading parameters. It is observed that the plots follow the exact PDF for a wide range of instantaneous SNRs. The multipath parameter $n$ determines the slope of the power PDF at $\gamma \to 0$. However, as the shadowing parameter $m_s$ and the average SNR are changed, there is a parallel shift in the figure.

*2) EGC diversity PDF:* Similar to MRC, the signals gleaned from $L$ paths are co-phased, weighted with a factor of unity and then are summed to get the combiner's output SNR as given below

$$\gamma_{EGC} = \left(\frac{1}{\sqrt{L}}\sum_{r=1}^{L}\sqrt{\gamma_r}\right)^2. \tag{12}$$

Taking the square root of both sides, yields

$$X_{EGC} = \sum_{r=1}^{L}\frac{X_r}{\sqrt{L}}. \tag{13}$$

Similarly to MRC, the MGF is expressed as

$$M_{X_{EGC}}(s) = \prod_{r=1}^{L} M_{X_r}\left(\frac{s}{\sqrt{L}}\right). \tag{14}$$

The envelope PDF for (3) is deduced by using the relationship of $P_Y(\gamma) = \frac{P_R\left(\sqrt{\frac{\hat{r}^2\gamma}{\bar{\gamma}}}\right)}{2\sqrt{\frac{\gamma\bar{\gamma}}{\hat{r}^2}}}$ [50, Eq. 2.3], yielding

$$f_X(x) = \frac{2\mathcal{R}h_j\mathcal{T}^{\Omega}\bar{\gamma}^{\Omega+1}}{\hat{x}^{2\Omega+2}}x^{2\Omega+1}. \tag{15}$$

Taking the LT of (15) results in

$$M_X\left(\frac{s}{\sqrt{L}}\right) = \frac{2\mathcal{R}h_j\mathcal{T}^{\Omega}\bar{\gamma}^{\Omega+1}\Gamma(2\Omega+2)}{\hat{x}^{2\Omega+2}\left(\frac{s}{\sqrt{L}}\right)^{2\Omega+2}}. \tag{16}$$

TABLE V
$h_j$ VALUES FOR VARIOUS FOX'S H-FADING CHANNELS

| Channel | $\hat{m}$ | $h_j$ |
|---|---|---|
| Maxwell | 1 | $h_1$=1 |
| $\alpha-\mu$ | 1 | $h_1=\frac{\alpha}{2}$ |
| E G-G | 2 | $h_1=\xi\Gamma\left(\frac{\hat{r}_s\xi_s-\hat{r}\xi}{\xi_s}\right)$, $h_2=\xi_s\Gamma\left(\frac{\hat{r}\xi-\hat{r}_s\xi_s}{\xi}\right)$ |
| F-S $\mathcal{F}$ | 1 | $h_1=\Gamma(\hat{n}+\hat{m})$ |
| GBK | 2 | $h_1=\hat{\lambda}\Gamma(n_G-m_G)$, $h_2=\hat{\lambda}\Gamma(m_G-n_G)$ |
| $\alpha$-$\mu$/G | 2 | $h_1=\Gamma\left(\hat{k}-\mu+\frac{1}{\alpha}-1\right)$), $h_2=\Gamma\left(\mu-\hat{k}-\frac{1}{\alpha}+1\right)$) |
| SSS | 2 | $h_1=\Gamma(m_2-m_1)\Gamma(a_1+m_1)$, $h_2=\Gamma(m_1-m_2)\Gamma(a_1+m_2)$ |
| DSS | 2 | $h_1=\Gamma(m_2-m_1)\Gamma(a_2+m_1)\Gamma(a_1+m_1)$, $h_2=\Gamma(m_1-m_2)\Gamma(a_2+m_2)\Gamma(a_1+m_2)$ |
| Cascaded G-$K$ | 4 | $h_1=\Gamma(\tilde{m}_1-\tilde{m}_{s1})\Gamma(\tilde{m}_{s2}-\tilde{m}_{s1})\Gamma(\tilde{m}_2-\tilde{m}_{s1})$, $h_2=\Gamma(\tilde{m}_{s1}-\tilde{m}_1)\Gamma(\tilde{m}_{s2}-\tilde{m}_1)\Gamma(\tilde{m}_2-\tilde{m}_1)$, $h_3=\Gamma(\tilde{m}_{s1}-\tilde{m}_{s2})\Gamma(\tilde{m}_1-\tilde{m}_{s2})\Gamma(\tilde{m}_2-\tilde{m}_{s2})$, $h_4=\Gamma(\tilde{m}_{s1}-\tilde{m}_2)\Gamma(\tilde{m}_1-\tilde{m}_2)\Gamma(\tilde{m}_{s2}-\tilde{m}_2)$ |
| Gamma-Gamma | 3 | $h_1=\Gamma(\varsigma-\tilde{\xi}^2)\Gamma(\varpi-\tilde{\xi}^2)$, $h_2=\frac{\Gamma(\tilde{\xi}^2-\varsigma)\Gamma(\varpi-\varsigma)}{\Gamma(\tilde{\xi}^2+1-\varsigma)}$, $h_3=\frac{\Gamma(\tilde{\xi}^2-\varpi)\Gamma(\varsigma-\varpi)}{\Gamma(\tilde{\xi}^2+1-\varpi)}$ |
| $N$-Rayleigh | N | $h_i$=1; $1\leq j\leq N$ |
| $N$-Nakagami-$m$ | N | $h_i=\prod_{i=1,i\neq j}^{N}\Gamma(m_i-m_j)$; $1\leq j\leq N$ |
| $N$-GK | 2N | $h_1=\Gamma(m_1-\tilde{m}_{s1})\Gamma(m_2-\tilde{m}_{s1})\Gamma(\tilde{m}_{s2}-\tilde{m}_{s1})....\Gamma(\tilde{m}_{sN}-\tilde{m}_{s1})\Gamma(m_N-\tilde{m}_{s1})$; $h_2=\Gamma(\tilde{m}_{s1}-m_1)\Gamma(m_2-m_1)\Gamma(\tilde{m}_{s2}-m_1)....\Gamma(\tilde{m}_{sN}-m_1)\Gamma(m_N-m_1)$; $h_3=\Gamma(\tilde{m}_{s1}-\tilde{m}_{s2})\Gamma(m_1-\tilde{m}_{s2})\Gamma(m_2-\tilde{m}_{s2})....\Gamma(\tilde{m}_{sN}-\tilde{m}_{s2})\Gamma(m_N-\tilde{m}_{s2})$; $h_{2N-1}=\Gamma(\tilde{m}_{s1}-\tilde{m}_{sN})\Gamma(m_1-\tilde{m}_{sN})\Gamma(\tilde{m}_{s2}-\tilde{m}_{sN})....\Gamma(m_{N-1}-\tilde{m}_{sN})\Gamma(m_N-\tilde{m}_{sN})$; $h_{2N}=\Gamma(\tilde{m}_{s1}-m_N)\Gamma(m_1-m_N)\Gamma(\tilde{m}_{s2}-m_N)....\Gamma(m_{N-1}-m_N)\Gamma(\tilde{m}_{sN}-m_N)$ |
| $N$-Fisher | N | $h_j=\prod_{i=1,i\neq j}^{N}\Gamma(\hat{n}_i-\hat{n}_j)\prod_{i=1}^{N}\Gamma(\hat{n}_j-\hat{m}_i)$; $1\leq j\leq N$ |
| $N$-$\alpha$-$\mathcal{F}$ | N | $h_j=\prod_{i=1,i\neq j}^{N}\Gamma(\Upsilon_i-\Upsilon_j)\prod_{i=1}^{N}\Gamma(\Upsilon_j-\Phi_i)$; $1\leq j\leq N$ |

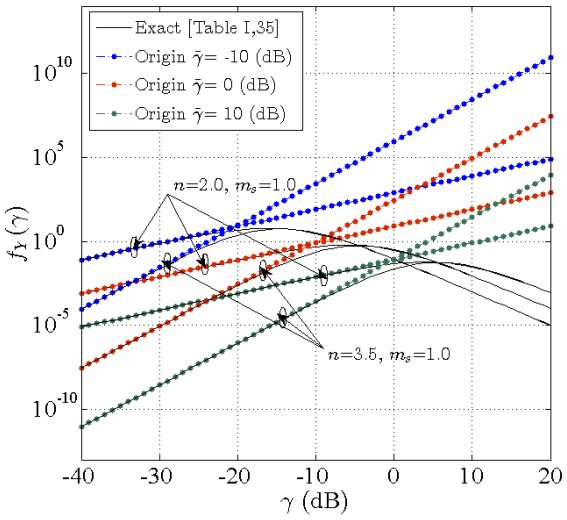


Fig. 1. Fisher-Snedecor $F$ distribution's origin and exact PDF.

Substituting (16) into (14) and carrying out some further algebraic manipulations yields

$$M_{X_{EGC}}(s)=\left\{\prod_{r=1}^{L}\left(\frac{2h_j\mathcal{R}_r\mathcal{T}^{\Omega_r}\bar{\gamma}_r^{\Omega+1}\Gamma(2\Omega_r+2)}{\hat{x}^{2\Omega_r+2}}\right)\right\}\times\frac{L^{\sum_{r=1}^{L}(\Omega_r+1)}\Gamma\left(\sum_{r=1}^{L}(2\Omega_r+2)\right)}{\Gamma\left(\sum_{r=1}^{L}(2\Omega_r+2)\right)s^{\sum_{r=1}^{L}(2\Omega_r+2)}}. \quad (17)$$

Taking the inverse LT of (16) yields the origin envelope PDF of EGC reception, where the independent paths are non-identical

$$f_{X_{EGC}}^{inid}(x) = \left\{ \prod_{r=1}^{L} \left( \frac{2h_j \mathcal{R}_r \mathcal{T}^{\Omega_r} \bar{\gamma_r}^{\Omega+1} \Gamma(2\Omega_r+2)}{\hat{x}^{2\Omega_r+2}} \right) \right\} \times \frac{L^{\sum_{r=1}^{L}(\Omega_r+1)} x^{\sum_{r=1}^{L}(2\Omega_r+2)-1}}{\Gamma\left( \sum_{r=1}^{L}(2\Omega_r+2) \right)}. \quad (18)$$

Finally, upon substituting the relationship given by [50, Eq. 2.3] into (18), the origin power PDF of EGC diversity reception is deduced similar by (10), where the parameters are defined in Table VI. Similarly to MRC, for i.i.d. the origin power PDF of EGC diversity reception will have a similar structure to (10) and the associated parameters are given in Table VI.

*3) SC diversity PDF:* In SC spatial diversity reception, the path having the highest SNR will be selected, thus the CDF is given by

$$F_{\gamma_{SC}}(\gamma) = \prod_{r=1}^{L} F_{\gamma_r}(\gamma). \quad (19)$$

Substituting (5) into (19) gives

$$F_{\gamma_{SC}}^{inid}(\gamma) = \left\{ \prod_{r=1}^{L} \left( \frac{\mathcal{R}_r h_j \mathcal{T}^{\Omega_r}}{\Omega_r+1} \right) \right\} \gamma^{\sum_{r=1}^{L}(\Omega_r+1)-1}. \quad (20)$$

To derive the PDF expression, the above relationship has to be differentiated with respect to the parameter $\gamma$. It yields the origin PDF of SC diversity similar to the origin MRC PDF given by (10). For i.i.d. scenarios, the PDF of SC diversity is given by

$$f_{Y_{SC}}^{iid}(\gamma) = L\left[F_Y(\gamma)\right]^{L-1} f_Y(\gamma). \quad (21)$$

Upon substituting (3) and (5) into (21), one can obtain the origin PDF expression for SC diversity similar to (10). In Table VI, the fading parameters are illustrated both for i.n.i.d. and i.i.d. cases.

## IV. Performance Metrics

Wireless communication systems have diverse performance metrics, such as the OP, the average SEP, the probability of missed detection, etc. Our research primarily focuses on high-power approximations of the performance metrics using the origin PDF. Therefore, we have evaluated the OP and average SEP performance metrics for both SIMO and SISO systems.

### A. Outage Probability

The OP describes the probability that the received SNR is below the minimum threshold ($\gamma_{th}$), which is formulated as [43]

$$P_{out}(\gamma_{th}) = P[\gamma < \gamma_{th}] = \int_0^{\gamma_{th}} f_Y(\gamma) d\gamma. \quad (22)$$

Upon substituting (10) into (22), after some manipulations, we get

$$P_{out}(\gamma_{th}) = \frac{\mathcal{K}^D \gamma_{th}^{\Psi^D}}{\Psi^D}, \quad (23)$$

where $D$ represents the MRC, EGC, and SC diversity parameters.

### B. Average SEP

Noise is one of the main sources of signal impediments in the communication system. The level of impact on the data transmission can be quantified by the average SEP. In this subsection, we will presented the analytical expressions of results for both the coherent and non-coherent detection based average SEP. The analytical representation of SEP under a fading environment is deduced by averaging i.e. integrating $P_e(\gamma)$ across the entire dynamic range of the fading PDF $f_Y(\gamma)$ [43, Eq. (12)]

$$\bar{P(e)} = \int_0^{\infty} P_e(\gamma) f_Y(\gamma) d\gamma, \quad (24)$$

where $P_e(\gamma)$ is the SEP of non-fading environments.

*1) Coherent average SEP:* Here, we will consider the scenario where phase recovery at the Rx is possible in the face of both AWGN and ALN.

*a) AWGN average SEP:* Under AWGN the SEP of a non-faded environment is given by [43, Eq. (13)]

$$P_e(\gamma) = \hat{\mathcal{A}} erfc(\sqrt{\hat{\mathcal{B}}\gamma}), \quad (25)$$

where the constant parameters $\hat{\mathcal{A}}$ and $\hat{\mathcal{B}}$ are associated with different coherent modulation schemes defined in [51, Table I]. Upon substituting (25) and (10) into (24) and setting $\sqrt{\hat{\mathcal{B}}\gamma} = r$, we get

$$\bar{P(e)} = \frac{2\hat{\mathcal{A}}\mathcal{K}^D}{\hat{\mathcal{B}}^{\Psi^D}} \int_0^{\infty} t^{2\Psi^D-1} erfc(t) dt. \quad (26)$$

Evidently, by the inclusion of [52, Eq. (2.8.2.1)], (26) can be simplified to

$$\bar{P(e)} = \frac{\hat{\mathcal{A}}\mathcal{K}^D}{\hat{\mathcal{B}}^{\Psi^D}\Psi^D\sqrt{\pi}} \Gamma\left( \frac{2\Psi^D+1}{2} \right). \quad (27)$$

*b) ALN average SEP:* Under ALN, the average SEP statistics discussed here are of BPSK, QPSK, and $M$-ary PSK. The transmitted signal is detected using the MED based detector, rather than a maximum likelihood detector. The MED detector is simple and its SEP expressions are of low complexity. The conditional SEP of BPSK and QPSK is formulated as

$$P_e(\gamma) = (a + b\sqrt{\gamma}) e^{-c\sqrt{\gamma}}, \quad (28)$$

where the constants $a$ and $b$ are defined in [20] and for the sake of completeness are reproduced here in Table VII. Upon substituting (10) and (28) into (24), as well as setting $\sqrt{\gamma} = t$, with the aid of [49, Eq. (3.381.4)], we have

$$\bar{P(e)} = \frac{2a\mathcal{K}^D\Gamma(2\Psi^D)}{c^{2\Psi^D}} + \frac{2b\mathcal{K}^D\Gamma(2\Psi^D+1)}{c^{2\Psi^D+1}}. \quad (29)$$

TABLE VI
DISTRIBUTION PARAMETERS FOR MRC, EGC, AND SC DIVERSITY SCHEMES

| Distribution Parameters | i.n.i.d. | i.i.d. |
|---|---|---|
| $\mathcal{K}^{MRC}$ | $\frac{\prod_{r=1}^{L}\left(\mathcal{R}_r h_j \mathcal{T}_r^{\Omega_r}\Gamma(\Omega_r+1)\right)}{\Gamma\left(\left(\sum_{r=1}^{L}\Omega_r\right)+L\right)}$ | $\frac{\mathcal{R}^L h_j^L \mathcal{T}^{L\Omega}\left(\Gamma(\Omega+1)\right)^L}{\Gamma\left(\Omega L+L\right)}$ |
| $\Psi^{MRC}$ | $\left(\sum_{r=1}^{L}\Omega_r\right)+L$ | $L\left(\Omega+1\right)$ |
| $\mathcal{K}^{EGC}$ | $\frac{\left\{\prod_{r=1}^{L}\left(2h_j\mathcal{R}_r\mathcal{T}_r^{\Omega_r}\Gamma(2\Omega_r+2)\right)\right\}L^{\sum_{r=1}^{L}(\Omega_r+1)}}{2\Gamma\left(\sum_{r=1}^{L}(2\Omega_r+2)\right)}$ | $\frac{\left(2h_j\mathcal{R}\mathcal{T}^{\Omega}\Gamma(2\Omega+2)\right)^L L^{L(\Omega+1)}}{2\Gamma((2\Omega+2)L)}$ |
| $\Psi^{EGC}$ | $\sum_{r=1}^{L}(\Omega_r+1)$ | $L(\Omega+1)$ |
| $\mathcal{K}^{SC}$ | $\left\{\sum_{r=1}^{L}(\Omega_r+1)\right\}\left\{\prod_{r=1}^{L}\left(\frac{\mathcal{R}_r h_j \mathcal{T}_r^{\Omega_r}}{\Omega_r+1}\right)\right\}$ | $L\frac{\left(\mathcal{R}h_j\mathcal{T}^{\Omega}\right)^L}{(\Omega+1)^{L-1}}$ |
| $\Psi^{SC}$ | $\sum_{r=1}^{L}(\Omega_r+1)$ | $L(\Omega+1)$ |

TABLE VII
SEP PARAMETERS FOR ADDITIVE LAPLACIAN NOISE

| Modulation Scheme | $a$ | $b$ | $c$ |
|---|---|---|---|
| BPSK | $\frac{1}{2}$ | 0 | 2 |
| QPSK | $\frac{3}{4}$ | 1 | 2 |

The conditional SEP of $M$-ary PSK for $M \geq 8$ is given as [20, Eq. (7)]

$$P_e(\gamma) = \frac{8}{M}\sum_{r=0}^{\frac{M}{4}-1}\mathcal{G}(r,\gamma) + \frac{2tan\left(\frac{\pi}{M}\right)^2}{M\left(1-tan\left(\frac{\pi}{M}\right)^2\right)}e^{-2\sqrt{\gamma}}, \quad (30)$$

where

$$G(r,\gamma) = \frac{1}{2\mathcal{W}_1}\left(\mathcal{W}_1^2 e^{-\mathcal{K}_1\sqrt{\gamma}} - \mathcal{W}_2^2 e^{-\mathcal{K}_2\sqrt{\gamma}}\right) - \frac{sin\left(\frac{2\pi}{M}\right)}{8\left(cos\left(\frac{2\pi}{M}\right)+sin\left(\frac{4r\pi}{M}\right)\right)}e^{-\mathcal{K}_3\sqrt{\gamma}}, \quad (31)$$

with $\mathcal{W}_1 = cos\left((2r+1)\frac{\pi}{M}\right)$, $\mathcal{W}_2 = sin\left((2r+1)\frac{\pi}{M}\right)$, $\mathcal{K}_1 = \frac{-2sin\left(\frac{\pi}{M}\right)}{e^{cos\left((2r+1)\frac{\pi}{M}\right)}}$, $\mathcal{K}_2 = \frac{-2sin\left(\frac{\pi}{M}\right)}{e^{sin\left((2r+1)\frac{\pi}{M}\right)}}$, and $\mathcal{K}_3 = 2\sqrt{2}cos\left(\frac{2r\pi}{M}-\frac{\pi}{M}\right)$. Utilizing the methodology of BPSK and QPSK, the SEP of $M$-ary PSK is deduced as follows

$$\begin{aligned}P(\bar{e}) =& \frac{8\mathcal{K}}{M}\sum_{r=0}^{\frac{M}{4}-1}\frac{cos\left((2r+1)\frac{\pi}{M}\right)^2\Gamma(2\Psi)}{cos\left((2r+1)\frac{2\pi}{M}\right)\mathcal{K}_1^{2\Psi}} \\ &- \frac{8\mathcal{K}}{M}\sum_{r=0}^{\frac{M}{4}-1}\frac{sin\left((2r+1)\frac{\pi}{M}\right)^2\Gamma(2\Psi)}{cos\left((2r+1)\frac{2\pi}{M}\right)\mathcal{K}_2^{2\Psi}} \\ &- \frac{8\mathcal{K}}{M}\sum_{r=0}^{\frac{M}{4}-1}\frac{sin\left(\frac{2\pi}{M}\right)\Gamma(2\Psi)}{4\left(cos\left(\frac{2\pi}{M}\right)+sin\left(\frac{4r\pi}{M}\right)\mathcal{K}_3^{2\Psi}\right)} \\ &+ \frac{tan\left(\frac{\pi}{M}\right)^2\Gamma(2\Psi)}{M\left(1-tan\left(\frac{\pi}{M}\right)^2\right)2^{2\Psi-1}}.\end{aligned} \quad (32)$$

*2) Non-Coherent average SEP:* Coherent detection requires perfect phase and channel state information at the Rx, which is hard to acquire. Therefore, non-coherent detection emerges as a low-complexity design for wireless sensor and relay networks [53]. Additionally, it is particularly beneficial for high Doppler SAGIN scenarios [54]. Specifically, it is beneficial because it reduces the system complexity and cost by eliminating channel estimation. Hence, we have derived the analytical expression of binary frequency shift keying, differential phase shift keying, and $M$-ary phase shift keying. The conditional SEP expression of AWGN is given by [43, Eq. (18)]

$$P_e(\gamma) = \mathcal{A}_n e^{-\mathcal{B}_n\gamma}, \quad (33)$$

where the constants $\mathcal{A}_n$ and $\mathcal{B}_n$ are given in [43, Table 2]. Upon substituting (10) and (33) into (24), with the aid of [49,

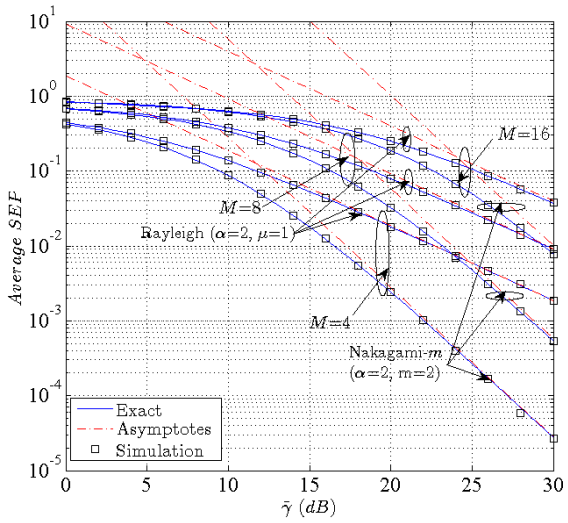


Fig. 2. Average SEP of $M$-ary PAM for special cases of $\alpha$-$\mu$ fading channel.

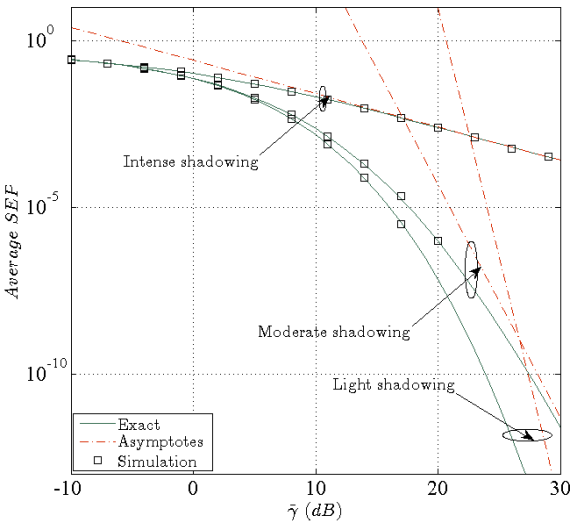


Fig. 3. Average BEP of BPSK for Fisher-$F$ fading under different shadowing with Additive Laplacian noise.

Eq. (3.381.4)], we arrive at

$$\bar{P(e)} \approx \frac{\mathcal{A}_n \mathcal{K}^D \Gamma(2\Psi^D)}{\mathcal{A}_n^{2\Psi^D}}. \tag{34}$$

### C. Diversity gain and SNR gain

Both the diversity gain and the SNR gain are important performance metrics that provide insights concerning the family of the diversity combining systems at high SNRs. The diversity gain determines the slope of the SEP curve, while the SNR gain measures the shift of the SEP curve relative to a benchmark SEP curve without changing its slope [11], [55], [56]. The SNR and diversity gains affect the OP and the average SEP as follows:

$$\begin{aligned} P_{out}(\gamma_{th}) &\approx \left(\mathcal{G}^{C_{op}}\bar{\gamma}\right)^{\mathcal{G}^{D_{op}}} \\ \bar{P}(e) &\approx \left(\mathcal{G}^{C_{Pe}}\bar{\gamma}\right)^{\mathcal{G}^{D_{Pe}}}, \end{aligned} \tag{35}$$

where the SNR and diversity gain parameters for the OP and average SEP are given by $\mathcal{G}^{C_{op}}$ & $\mathcal{G}^{C_{Pe}}$ and $\mathcal{G}^{D_{op}}$ & $\mathcal{G}^{D_{Pe}}$, respectively.

## V. Results and Discussions

The accuracy of the mathematical analysis presented in the previous sections requires validation. Hence, all the theoretical plots are compared to the Monte-Carlo simulation results with $\geq 10^6$ samples. Additionally, we also examine the impact of system parameters through different performance metrics, such as the OP and average SEP/BEP for a few special cases of Fox's H-functions, namely for the $\alpha$-$\mu$, Fisher-Snedecor $F$, GBK, and single shadowed scenarios.

In Fig. 2, the average SEP of coherent $M$-ary PAM has been plotted for the $\alpha$-$\mu$ fading model. The figure contains exact (generated through integral simulation), asymptotic, and simulation results. To elaborate, Fig. 2 includes two special cases, namely the Rayleigh ($\alpha$=2 & $\mu$) and Nakagami-$m$ ($\alpha$=2 & $m$=2$\mu$) scenarios, for $M$=4, 8, and 16 conveying 2, 3, and 4 bits. The figure clearly demonstrates that as expected, an increase in the constellation size increases the SEP, the intra-constellation distance is reduced. It is further noted that the asymptotes coincide with the exact and simulation results.

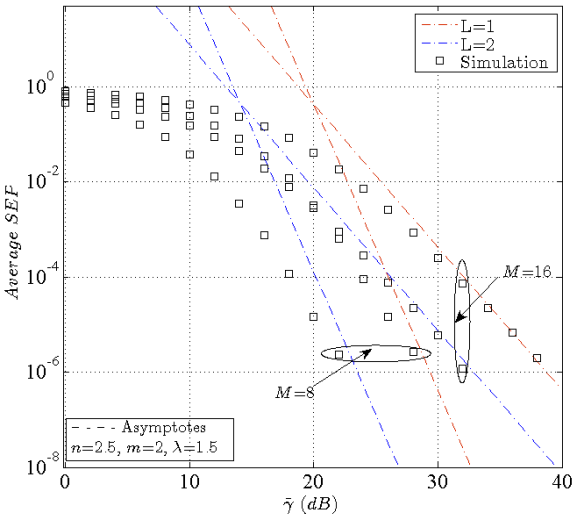


Fig. 4. Average SEP of $M$-ary PSK for GBK distribution with MRC diversity.

Figure 3 shows the average BEP for binary phase shift keying in the face of ALN for transmission over Fisher-Snedecor $F$ distributed fading channels. The set of values considered for the Fisher-Snedecor $F$ parameters $n$ and $m_s$ are in the range of $1 \rightarrow 15$. The figure includes plots for three special shadowing cases, such as intense shadowing ($n$=1, $m_s$=1), moderate shadowing ($n$=7, $m_s$=7), and light shadowing ($n$=15, $m_s$=15). As expected, shadowing has an adverse effect on the system. The SEP of $10^{-5}$ is achieved at about 16 (dB) for light shadowing, nearly 18 (dB) for moderate shadowing, and at a very high SNR beyond 30 (dB) for intense shadowing.

The average SEP plots for MRC and SC diversity are illustrated in Figs. 4 and 5. Explicitly, Fig. 4 plots the SEP of

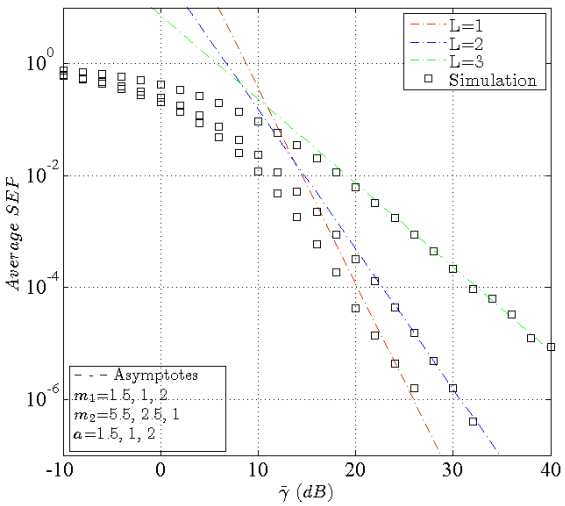


Fig. 5. Average SEP of QPSK for SSS distribution with i.n.i.d. distributed branches.

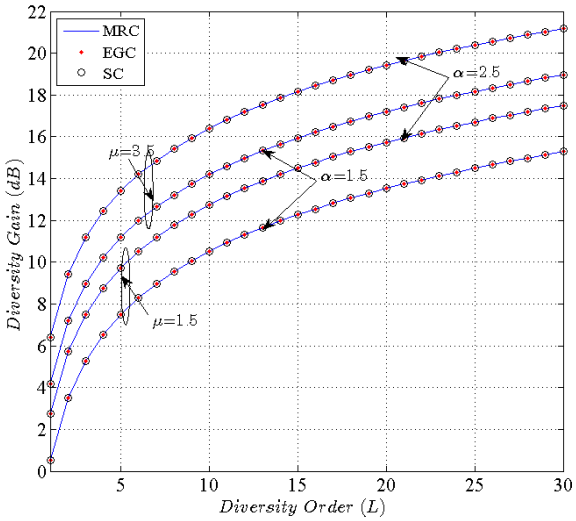


Fig. 7. Diversity gain of OP versus $L$ for $\alpha$-$\mu$ fading with varying fading parameters.

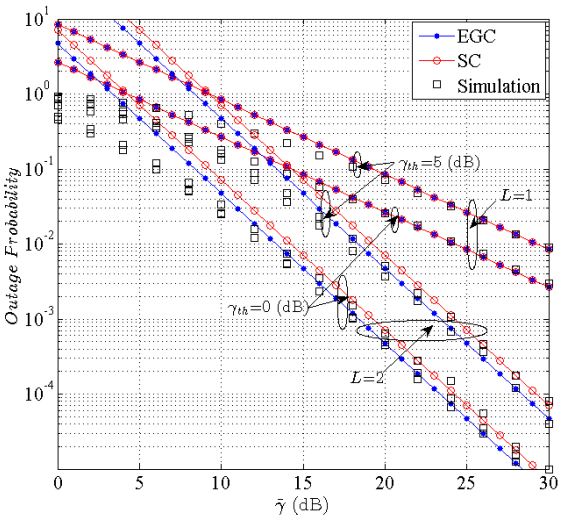


Fig. 6. Outage probability for $N$ cascaded Nakagami-$m$ fading.

$M$-ary phase shift keying for transmission over GBK channels. Here, two i.i.d. branches are considered, and the parameters are as follows: $n$=2.5, $m$=2, $\lambda$=1.5, for constellation sizes of $M$=8 & 16. As expected, the increasing number of diversity branches improves the system's reliability. For example, to achieve SEP of $10^{-4}$, SNRs of 25 (dB) and 18 (dB) are required for diversity orders of $L$=1 and $L$=2 respectively at $M$=8. Similarly, SNRs of 32 (dB) and 27 (dB) are required for diversity orders of $L$=1 and $L$=2 at $M$=16. It is further noted in Fig. 4 that a comparatively higher shift in SNR ($\sim$ 7 (dB)) is achieved at $M$=8, while $\sim$ 5 (dB) will be observed for $M$=16.

In Fig. 5, the average SEP plot for QPSK modulation scheme versus average SNR is plotted for the transmission over SSS model using SC diversity. Under this case, the individual branches are considered to be i.n.i.d., where $m_1$=$\{1.5, 1, 2\}$, $m_2$=$\{5.5, 2.5, 1\}$, $a$=$\{1.5, 1, 2\}$, and $L$=$\{1, 2, 3\}$. We observe that the error probability decreases upon increasing the diversity order. This is because as the number diversity paths increases, the combiner selects the specific path having the highest SNR. For example, to arrive at a SEP of $10^{-4}$, the system having a single branch requires an average SNR of 28 (dB), while a dual-branch system requires an SNR of $\sim$22 (dB), and a triple-branch system needs 20 (dB). This explains why the initial diversity order increment has a significant contribution to the performance enhancement attained.

EGC and SC diversity schemes. The parameters considered here are as follows: $m_1$=1.5, $m_2$=1, threshold SNR, i.e., $\gamma_{th}$=0 (dB) & 5 (dB), and the number of diversity paths is $L$=2 & 3. The OP is typically reduced as the number of antennas at the Rx increases. This is due to the fact that systems with multiple antennas have higher SNR. It is further observed that the OP of EGC diversity is lower than that of SC diversity and it increases as the threshold SNR increases. For example, at an average SNR of 30 (dB), the probability of outage is $9\times10^{-3}$ with $\gamma_{th}$=5 (dB) and $2.9\times10^{-3}$ with $\gamma_{th}$=0 (dB), respectively. In all the plots, it has been verified that the asymptotes are in good agreement with the simulations at high SNRs, but depends on the choice of the fading parameters.

Fig. 7 depicts the plot of diversity gain against diversity order. The analytical expression for the diversity gain is given by $\mathcal{G}^{D_{op}}$=$L(\Omega+1)$. It is observed from the plot and the expressions that all the diversity combining schemes have the same representation of diversity gain and are also independent of the OP threshold. It is further observed that the diversity gain increases as the fading parameters $\alpha$ and $\mu$ increase.

## VI. Summary and Conclusion

Unified average SEP and OP results have been presented for generalised Fox's H-fading with spatial diversity. The entire body of work presented is based on the origin PDF, which produces performance results at a reduced complexity. The work also addressed the parameters of the origin PDF for some special cases of Fox's H-fading that are well

suited for different wireless applications, namely, inter-vehicle communication, unmanned aerial communication, millimetre wave communication, etc. All the formulations derived are compared to numerical simulation results to quantify their precision.

## REFERENCES


[1] Y. Abo Rahama, M. H. Ismail and M. S. Hassan, "On the Sum of Independent Fox's H-Function Variates With Applications," *IEEE Transactions on Vehicular Technology*, vol. 67, no. 8, pp. 6752–6760, Aug. 2018, doi: 10.1109/TVT.2018.2827180.

[2] M. M. H. El Ayadi and M. H.Ismail, "Unified Approach for Probability of Detection Evaluation Over Generalised Fading Channels," *IET Communication*, vol. 10, no. 12, pp. 1532–1541, 2016.

[3] Y. Jeong, J. W. Chong, H. Shin and M. Z. Win, "Inter-vehicle Communication: Cox-Fox Modeling," *IEEE Journal on Selected Areas in Communications*, vol. 31, no. 9, pp. 418–433, Sept. 2013, doi: 10.1109/JSAC.2013.SUP.0513038.

[4] Y. Aborahama, M. H. Ismail and M. S. Hassan, "Novel Methods for Generating Fox's H-Function Distributed Random Variables With Applications," *IEEE Transactions on Vehicular Technology*, vol. 68, no. 7, pp. 7150–7154, July 2019, doi: 10.1109/TVT.2019.2916385.

[5] S. K. Yoo, S. L. Cotton, P. C. Sofotasios, M. Matthaiou, M. Valkama and G. K. Karagiannidis, "The Fisher-Snedecor $F$ Distribution: A Simple and Accurate Composite Fading Model," *IEEE Communications Letters*, vol. 21, no. 7, pp. 1661–1664, July 2017.

[6] F. Yilmaz and M. S. Alouini, "A Novel Unified Expression for the Capacity and Bit Error Probability of Wireless Communication Systems Over Generalized Fading Channels," *IEEE Transactions on Communications*, vol. 60, no. 7, pp. 1862–1876, July 2012, doi: 10.1109/TCOMM.2012.062512.110846.

[7] Y. Abo Rahama,M.H. Ismail,M.S. Hassan, "Capacity of Fox's H-function Fading Channel With Adaptive Transmission," *Electronics Letter*, vol. 52 , no. 11, pp. 976–978, May 2016, https://doi.org/10.1049/el.2016.0511.

[8] Z. Ji, C. Dong, Y. Wang and J. Lu, "On the Analysis of Effective Capacity Over Generalized Fading Channels," *2014 IEEE International Conference on Communications (ICC)*, 2014, pp. 1977–1983, doi: 10.1109/ICC.2014.6883613.

[9] L. Kong, G. Kaddoum and H. Chergui, "On Physical Layer Security Over Fox's H-Function Wiretap Fading Channels," *IEEE Transactions on Vehicular Technology*, vol. 68, no. 7, pp. 6608–6621, July 2019, doi: 10.1109/TVT.2019.2915017.

[10] P. S. Chauhan, S. Kumar, V. K. Upaddhyay, R. Mishra, B. Kumar, S. K. Soni, "Performance Analysis of ED Over Air-to-ground and Ground-to-ground Fading Channels: A unified and exact solution," *International Journal of Electronics and Communications (AEU)*, vol. 138, pp. 153839, 2021, https://doi.org/10.1016/j.aeue.2021.153839.

[11] Z. Wang and G. B. Giannakis, "A simple and General Parameterization Quantifying Performance in Fading Channels," *IEEE Transactions on Communications*, vol. 51, no. 8, pp. 1389–1398, Aug. 2003, doi: 10.1109/TCOMM.2003.815053.

[12] F. R. A. Parente and J. C. S. S. Filho, "Asymptotically Exact Framework to Approximate Sums of Positive Correlated Random Variables and Application to Diversity-Combining Receivers," *IEEE Wireless Communications Letters*, vol. 8, no. 4, pp. 1012–1015, Aug. 2019, doi: 10.1109/LWC.2019.2904032.

[13] B. Zhu, J. Cheng, J. Yan, J.-y. Wang, L. Wu and Y. Wang, "A New Asymptotic Analysis Technique for Diversity Receptions Over Correlated Lognormal Fading Channels," *IEEE Transactions on Communications*, vol. 66, no. 2, pp. 845–861, Feb. 2018, doi: 10.1109/TCOMM.2017.2767039.

[14] A. S. Gvozdarev, "Closed-Form and Asymptotic BER Analysis of the Fluctuating Double-Rayleigh With Line-of-Sight Fading Channel," *IEEE Wireless Communications Letters*, vol. 11, no. 7, pp. 1548–1552, July 2022, doi: 10.1109/LWC.2022.3179900.

[15] A. Wojnar, "Unknown Bounds on Performance in Nakagami Channels," *IEEE Transactions on Communications*, vol. 34, no. 1, pp. 22-24, Jan. 1986.

[16] H. Hashemi, J. Haghighat, M. Eslami and W. A. Hamouda, "Analysis of Equal Gain Combining Over Fluctuating Two-Ray Channels With Applications to Millimeter-Wave Communications," *IEEE Transactions on Vehicular Technology*, vol. 69, no. 2, pp. 1751–1765, Feb. 2020, doi: 10.1109/TVT.2019.2959877.

[17] H. Li, Y. Wang, F. Guo, J. Wang, B. Wang, and C. Wu, "Security and Privacy Challenges for Internet-of-Things and Fog Computing 2021," *Wireless Communications and Mobile Computing*, July 2021, https://doi.org/10.1155/2021/4696455.

[18] H. Soury and M.-S. Alouini, "On the Symbol Error Rate of $M$-ary MPSK over Generalized Fading Channels with Additive Laplacian Noise," *in Proc. IEEE International Symposium on Information Theory*, 2014, pp. 2879– 2883, doi: 10.1109/ISIT.2014.6875360.

[19] H. Soury and M. Alouini, "Symbol Error Rate of MPSK Over EGK Channels Perturbed by a Dominant Additive Laplacian Noise," *in IEEE Transactions on Communications*, vol. 63, no. 7, pp. 2511–2523, July 2015, doi: 10.1109/TCOMM.2015.2438813.

[20] O. S. Badarneh, "Error Rate Analysis of $M$-ary Phase Shift Keying in $\alpha$-$\eta$-$\mu$ Fading Channels Subject to Additive Laplacian Noise," *IEEE Communications Letters*, vol. 19, no. 7, pp. 1253–1256, July 2015, doi: 10.1109/LCOMM.2015.2423277.

[21] T. B. Santoso and M. Huda, "Performance Analysis of BPSK System in the Underwater Acoustic Channel with Additive Laplacian Noise," *2017 International Electronics Symposium on Engineering Technology and Applications (IES-ETA)*, 2017, pp. 75–80, doi: 10.1109/ELECSYM.2017.8240382.

[22] L. Kong, G. Kaddoum and Z. Rezki, "Highly Accurate and Asymptotic Analysis on the SOP Over SIMO $\alpha$-$\mu$ Fading Channels," *IEEE Communications Letters*, vol. 22, no. 10, pp. 2088–2091, Oct. 2018, doi: 10.1109/LCOMM.2018.2861877.

[23] P. S. Chauhan, S. Kumar, V. K. Upaddhyay and S. K. Soni, "Unified Approach to Effective Capacity for Generalised Fading Channels," *Physical Communication*, vol. 45, 101278, April 2021.

[24] X. Wang, W. Cheng and X. Xu, "On the Exact and Asymptotic Analysis of Wireless Transmission over $\alpha$-$\mu$/Inverse Gamma Composite Fading Channels," *2020 International Conference on Wireless Communications and Signal Processing (WCSP)*, 2020, pp. 789–794.

[25] R. Maurya, P. S. Chauhan, S. Srivastava, S.K. Soni and B. Mishra, "Energy Detection Investigation Over Composite $\alpha$-$\mu$/inverse-gamma Wireless Channel," *International Journal of Electronics and Communications (AEU)*, vol. 130, 153556, Feb. 2021.

[26] P. S. Chauhan, S. Kumar and S. K. Soni, "Performance Analysis of Non-identical Cascaded $\alpha$-$\mu$ Fading Channels," *Wireless Personal Communications*, vol. 116, pp. 3553–3566, 2021.

[27] A. M. Magableh, T. Aldalgamouni, O. Badarneh, S. Mumtaz, and S. Muhaidat, "Performance of Non-Orthogonal Multiple Access (NOMA) Systems over N-Nakagami-$m$ Multipath Fading Channels for 5G and Beyond," *IEEE Transactions on Vehicular Technology*, vol. 71, no. 11, pp. 11615–11623, Nov. 2022, doi: 10.1109/TVT.2022.3189589.

[28] A. A. Khuwaja, Y. Chen, N. Zhao, M. S. Alouini, P. Dobbins, "A Survey of Channel Modeling for UAV Communications," *IEEE Communication Survey & Tutorials*, vol. 20, no. 4, pp. 2804–2820, 2018.

[29] F. Yilmaz and M. S. Alouini, "A New Simple Model for Composite Fading Channels: Second Order Statistics and Channel Capacity," *2010 7th International Symposium on Wireless Communication Systems*, 2010, pp. 676–680, York, UK.

[30] A. Mathai, R. K. Saxena, and H. J. Haubold, *The H-function: Theory and Applications*, 1st Edn., Springer; 2010.

[31] O. S. Badarneh, "Statistics of the Product of Two $\alpha$-$\mathcal{F}$ Variates With Applications," *in IEEE Communications Letters*, vol. 25, no. 6, pp. 1761–1765, June 2021, doi: 10.1109/LCOMM.2021.3062598.

[32] A. P. Prudnikov, Y. A. Brychkov, and O. I. Marichev O I, *Integrals and Series 1st Edn. More Special Functions vol. 3*, Gordon and Breach Science Publishers; 1986.

[33] P. S. Chauhan, V. Rana, *et al.*, "Performance Analysis of Wireless Communication System Over Non-identical Cascaded Generalised Gamma Fading Channels," *International Journal of Communication Systems*, vol. 32, e4004, 2019. https://doi.org/10.1002/dac.4004.

[34] O. S. Badarneh, "Performance Evaluation of Wireless Communication Systems Over Composite $\alpha$-$\mu$/Gamma Fading Channels," *Wireless Personal Communication*, vol. 17, pp. 1235–1249, 2017.

[35] X. Chen, X. Hu, Q. Zhu, W. Zhong, and B. Chen, "Channel Modeling and Performance Analysis for UAV Relay Systems," *China Communications*, vol. 15, no. 12, pp. 89–97, Dec. 2018

[36] P. S. Bithas, V. Nikolaidis, A. G. Kanatas, and G. K. Karagiannidis, "UAV-to-ground Communications: Channel Modeling and UAV Selection," *IEEE Transactions on Communications*, vol. 68, no. 8, pp. 5135–5144, Aug. 2020

[37] I. S. Ansari, F. Yilmaz and M. Alouini, "Performance Analysis of FSO Links Over Unified Gamma-Gamma Turbulence Channels," *2015 IEEE 81st Vehicular Technology Conference (VTC Spring)*, pp. 1–5, 2015.

[38] P. C. Sofotasios, L. Mohjazi, S. Muhaidat, M. Al-Qutayri and G. K. Karagiannidis, "Energy Detection of Unknown Signals Over Cascaded Fading Channels," *IEEE Antennas and Wireless Propagation Letters*, vol. 15, pp. 135–138, 2016.

[39] G. K. Karagiannidis, N. C. Sagias and P. T. Mathiopoulos, "$N*$Nakagami: A Novel Stochastic Model for Cascaded Fading Channels," *in IEEE Transactions on Communications*, vol. 55, no. 8, pp. 1453–1458, Aug. 2007.

[40] I. Trigui, A. Laourine, S. Affes and A. Stephenne, "On the Performance of Cascaded Generalized K Fading Channels," *GLOBECOM 2009 - 2009 IEEE Global Telecommunications Conference*, 2009, pp. 1–5.

[41] O. S. Badarneh, S. Muhaidat, P. C. Sofotasios, S. L. Cotton, K. Rabie and D. B. da Costa, "The $N*$Fisher-Snedecor F Cascaded Fading Model," *2018 14th International Conference on Wireless and Mobile Computing, Networking and Communications (WiMob)*, 2018, pp. 1–7.

[42] P. S. Chauhan, and S. K. Soni, "Performance Analysis of Dual Branch MRC Diversity Over Non-identical Mixture of Gamma Distribution," *5th IEEE Uttar Pradesh Section International Conference on Electrical, Electronics and Computer Engineering (UPCON)*, pp. 1–4, 2018; Gorakhpur, India.

[43] P. S. Chauhan, D. Tiwari, and S. K. Soni, "New Analytical Expressions for the Performance Metrics of Wireless Communication System Over Weibull/Lognormal Composite Fading," *International Journal of Electronics and Communications (AEU)* vol. 82, pp. 397–405, 2017.

[44] P. S. Chauhan, P. Negi, S. K. Soni, "A Unified Approach to Modelling of Probability of Detection Over $\alpha$-$\mu$/IG, $\kappa$-$\mu$/IG, and $\eta$-$\mu$/IG Composite Fading Channels With Application to Cooperative System," *International Journal of Electronics and Communications (AEU)*, vol. 87, pp. 33–42, 2017.

[45] S. Kumar, P. S. Chauhan, P. Raghuvanshi, and M. Kaur, "ED Performance Over $\alpha$-$\eta$-$\mu$/IG and $\alpha$-$\kappa$-$\mu$/IG Generalized Fading Channels With Diversity Reception and Cooperative Sensing: A Unified Approach," *International Journal of Electronics and Communications (AEU)*, vol. 97, pp. 273-279, 2018. https://doi.org/10.1016/j.aeue.2018.10.027

[46] K. P. Peppas, G. Efthymoglou, V. A. Aalo, M. Alwakeel, and S. Alwakeel, "Energy Detection of Unknown Signals in Gamma-shadowed Rician Fading Environments With Diversity Reception," *IET Communication*, vol. 9, no. 2, pp. 196–210, January 2015.

[47] A. A. Kilbas, *On the H-function*. https://arxiv.org/abs/math/9803163.

[48] P. S. Chauhan, S. Kumar, S. K. Soni, "New Approximate Expressions of Average Symbol Error Probability, Probability of Detection and AUC With MRC Over Generic and Composite Fading Channels," *International Journal of Electronics and Communications (AEU)*, vol. 99, pp. 119–129, 2019.

[49] I. S. Gradshteyn and I. M. Ryzhik, *Table of Integrals, Series, and Products*, 6th ed. New York, Academic Press; 2000.

[50] M. K. Simon and M. S. Alouini, *Digital Communication Over Fading Channels: A Unified Approach to Performance Analysis*, John Wiley & Sons, 2000.

[51] O. S. Badarneh and M. S. Aloqlah, "Performance Analysis of Digital Communication Systems Over $\alpha$-$\eta$-$\mu$ Fading Channels," *IEEE Transactions on Vehicular Technology*, vol. 65, no. 10, 7972–7981, October 2016. https://doi.org/10.13140/RG.2.1.4046.7925

[52] A. P. Prudnikov, Y. A. Brychkov, and O. I. Marichev, *Integrals and Series Volume 2: Special Functions* ($1^{st}$ Edn.). Gordon and Breach Science Publishers; 1986.

[53] B. Selim *et al.*, "Performance Analysis of Coherent and Non-coherent Modulation Under I/Q Imbalance Effects," *IEEE Access*, vol. 9, pp. 36125–36139, 2021, doi: 10.1109/ACCESS.2020.3028869.

[54] C. Xu et al., "Sixty Years of Coherent Versus Non-Coherent Tradeoffs and the Road From 5G to Wireless Futures," *IEEE Access*, vol. 7, pp. 178246–178299, 2019, doi: 10.1109/ACCESS.2019.2957706.

[55] B. Zhu, J. Yan, Y. Wang, L. Wu and J. Cheng, "Asymptotically Tight Performance Bounds of Diversity Receptions Over $\alpha$-$\mu$ Fading Channels With Arbitrary Correlation," *IEEE Transactions on Vehicular Technology*, vol. 66, no. 9, pp. 7619–7632, Sept. 2017, doi: 10.1109/TVT.2017.2686700.

[56] H. Ding, J. Ge, D. B. da Costa and Z. Jiang, "Asymptotic Analysis of Cooperative Diversity Systems With Relay Selection in a Spectrum-Sharing Scenario," *IEEE Transactions on Vehicular Technology*, vol. 60, no. 2, pp. 457–472, Feb. 2011, doi: 10.1109/TVT.2010.2100053.


**PUSPRAJ SINGH CHAUHAN** was born in UP, India. He received his Bachelor of Technology in Electronics and Communication Engineering from Uttar Pradesh Technical University, India in 2009, the M. Tech. degree in Digital Signal Processing from Govind Ballabh Pant Engineering College, Pauri, Uttarakhand, India in 2011, and Ph. D. degree in wireless communication in 2021. Currently he is working as Assistant Professor at Pranveer Singh Institute Of Technology, Kanpur, U.P., India. He also received best paper award at UPCON 2018, Gorakhpur. His research interests include wireless communication, propagation channel modeling, internet of things. He is also serving various international journals as reviewers, such as IEEE, Elsevier, Springer, Willey.

**SANDEEP KUMAR** (M'19-SM'22) received his B. Tech. in electronics and communication from Kurukshetra University, India in 2004 and Master of Engineering in Electronics and Communication from Thapar University, Patiala, India in 2007. He received his Ph.D. from Delhi Technological University, Delhi, India in 2018. He is currently working as Member (Senior Research Staff) at Central Research Laboratory, Bharat Electronics Limited Ghaziabad, India. He has received various awards and certificates of appreciation for his research activities. His research interests include the study of wireless channels, performance modeling of fading channels and cognitive radio networks. He is also serving as a reviewer for IEEE, Elsevier and Springer journals.

**ANKIT JAIN** has received his Bachelor of Technology in Electronics and Instrumentation Engineering from Uttar Pradesh Technical University, India in 2007 and M.Tech. in Electronics Instrumentation and Control Engineering with honours from NITTTR, Chandigarh. Currently, he is working as an Assistant Professor in the Department of Electronics and Communication at PSIT, Kanpur. He has two patents granted in his credit. His main area of research is embedded systems and Internet of things (IoT), wireless communication.

**LAJOS HANZO**
http://www-mobile.ecs.soton.ac.uk,
https://en.wikipedia.org/wiki/Lajos_Hanzo
(FIEEE'04) received Honorary Doctorates from the Technical University of Budapest and Edinburgh University. He is a Foreign Member of the Hungarian Science-Academy, Fellow of the Royal Academy of Engineering (FREng), of the IET, of EURASIP and holds the IEEE Eric Sumner Technical Field Award.